ELSEVIER

Biophysical Chemistry 118 (2005) 57 – 68

Biophysical Chemistry

http://www.elsevier.com/locate/biophyschem

Simulation of the influences of bathing solution and crosslink density on the swelling equilibrium of ionic thermo-sensitive hydrogels

Hua Li *, Zijie Wang, Xiaogui Wang, K.Y. Lam

Institute of High Performance Computing, National University of Singapore, 1 Science Park Road, #01-01 The Capricorn, Singapore Science Park II, Singapore 117528

Received 23 April 2005; received in revised form 7 July 2005; accepted 8 July 2005
Available online 1 August 2005

Abstract

The influences of the bathing solution and crosslink density on the swelling equilibrium of ionic thermo-sensitive hydrogels due to temperature stimulus are studied by mathematical modeling. The model used is termed the multi-effect-coupling thermal-stimulus (MECtherm) model with consideration of multiphases and multiphysics. It is used for the steady-state numerical simulation of the hydrogels in swelling equilibrium after it is verified well by comparison with available experimental data concerning the variation of volume swelling ratio with temperature. The phenomenon of volume phase transition is simulated for the thermal-stimulus responsive hydrogel. Simulations predict well the influences of the bathing solution concentration and crosslink density of polymeric network on the swelling equilibrium of the hydrogels.

Keywords: Thermally responsive hydrogel; Modeling; Swelling; Bathing solution; Crosslink density

1. Introduction

Currently the applications of stimuli-responsive hydrogels as critically active elements are explored intensively in various BioMEMS devices/systems due to their good sensitivity to surrounding environmental conditions such as temperature, salt concentration, solution pH and electric field [1–5]. Some of them immersed in solution can undergo a continuous or discontinuous volume phase transition which is characterized by a large change in swelling degree due to small change of environmental conditions. Hydrogels may thus be classified by sensitivity to different environmental stimuli.

Thermo-sensitive hydrogel is one of stimuli-responsive hydrogels, in which the poly(*N*-isopropylacrylamide) (PNIPA) and its copolymers are the typical thermo-sensitive hydrogels. They have attracted considerable interest [6] because of their intrinsic characteristics of very large volume change near the lower critical solution temperature (LCST). When surrounding temperature is below LCST, the hydrogel is in swollen state by absorbing solvent from surrounding solution. If above LCST, it is in shrunken state through exuding the solvent. In general, the volume phase transition results from the competitive balance between repulsive and attractive interactions [7]. According to the Flory's mean field theory for analysis of the swelling equilibrium of hydrogels [8], the interactions may be mathematically presented by three contributions to the change of free energy, namely the polymer–solvent mixing, elastic deformation of polymeric network matrix and osmotic pressure due to ionic concentration difference. The polymer–solvent mixing contributes to either attractive or repulsive forces, depending on the relation between entropy change and heat associated with the mixing. The elastic deformation of polymeric network matrix is balanced by mechanical restoring force of the matrix due to material elasticity. The osmotic pressure is one of the driving sources for expansion, as the result of ionic concentration difference

* Corresponding author. Tel.: +65 64191249; fax: +65 64191280.
E-mail address: lihua@ihpc.a-star.edu.sg (H. Li).

0301-4622/$ - see front matter © 2005 Elsevier B.V. All rights reserved.
doi:10.1016/j.bpc.2005.07.002

between the interior hydrogels and exterior bathing solution. According to the thermodynamic equilibrium theorem, the thermal-stimulus responsive hydrogels reach to the swelling equilibrium state when the three forces are balanced with each other. In addition, several important interactions are usually considered in analysis of the volume phase transition of the hydrogels. They include the hydrophobic, electrostatic, hydrogen-bond and van der Waals interactions [9]. It is also noted that the charged groups attached to the polymer chains play an essential role in the volume phase transition of the ionized hydrogels [10]. Therefore, the volume phase transition of thermo-sensitive hydrogels may be predicted by mathematical modeling based on thermodynamic equilibrium theorem.

However, the literature search shows that so far most of studies concerning the thermal-stimulus responsive hydrogels were experiment-based. Few studies of modeling and simulation were conducted. They include the early work on the statistical thermodynamic model presented by Lele et al. with consideration of hydrogen bond interaction in the swelling equilibrium of PNIPA hydrogel immersed into water [11]. Otake et al. developed the model with effects of hydrophobic hydration and interaction for analysis of the thermally induced discontinuous shrinkage of ionized hydrogels [12]. Erman and Flory studied discontinuous volume phase transition by assuming the parameters detailing the polymer–solvent interaction to be dependent on the volume fraction of polymeric network solid-phase matrix [13]. Hino and Prausnitz proposed a molecular thermodynamic model [14] by combing the compressible lattice-gas model [15] with the interpolated affine model [16] for simulation of volume phase transition of the PNIPA hydrogels. However, it is still difficult for these mentioned models to quantitatively predict the response behaviors of thermo-sensitive hydrogels, especially compared with experimental data. In order to overcome the shortcomings, the present authors developed a multiphysics model, called the multi-effect-coupling thermal-stimulus (MECtherm) model, with chemo-electro-thermo-mechanical energy domains [17]. In the model, the steady-state Nernst–Planck nonlinear partial differential equations and Poisson equation describe the diffusive ionic species and electric potential. According to the Flory's mean field theory, the transcendental governing equation of swelling equilibrium considers the three fundamental contributions mentioned, the polymer–solvent mixing, elastic deformation of polymeric network matrix and osmotic pressure due to ionic concentration difference. The model is validated to predict well the volume phase transition of swelling equilibrium of thermal-stimulus responsive hydrogels.

This paper will use the MECtherm model for further analysis of influences of the bathing solution concentration and polymeric-network crosslink density on the swelling equilibrium of the hydrogels and on the variation of volume phase transition with temperature, mobile ion concentrations and electric potential for the ionic hydrogels immersed in solution. The present ionic hydrogels are considered as a triphase hydrophilic mixture consisting of ionic phase, interstitial liquid phase and three-dimensional charged solid matrix phase of crosslinked polymeric-chain network. The MECtherm model, consisting of nonlinear partial differential equations coupled with a transcendental equation, will be solved by the truly meshless Hermite–cloud method [18] for one-dimensional simulation of swelling equilibrium of cylindrical thermo-sensitive hydrogels with volume phase transition when immersed in a bathing solution. The model is examined numerically by comparison with experimental data. Then, the simulations conducted predict the influences of the bathing solution concentration and polymeric-network crosslink density on the swelling equilibrium of the hydrogels with volume phase transition and on the distributions of mobile ion concentrations and fixed charge density as well as electric potential in both the hydrogels and surrounding bathing solution.

2. MECtherm model

According to the thermodynamic equilibrium theorem, the swelling equilibrium of ionized thermo-sensitive hydrogel may be determined by the initial and finial temperature fields and several parameters at reference state, including the fixed charge density, the effective crosslink density and the polymer-network volume fraction. By the Flory's mean field theory [8], the total change ΔG_{gel} of free energy of the hydrogels is expressed as

$$\Delta G_{\mathrm{gel}} = \Delta G_{\mathrm{Mixing}} + \Delta G_{\mathrm{Elastic}} + \Delta G_{\mathrm{Ion}}, \tag{1}$$

where $\Delta G_{\mathrm{Mixing}}$, $\Delta G_{\mathrm{Elastic}}$ and ΔG_{Ion} represent the polymer–solvent mixing, polymeric network elastic deformation and ionic contributions to the change of free energy, respectively. Differentiation of the above equation with respect to the number of solvent molecules in the hydrogel gives an expression of the total chemical potential ($\Delta\mu_{\mathrm{gel}}$) of the hydrogel due to the mixing ($\Delta\mu_{\mathrm{Mixing}}$), polymer elastic deformation ($\Delta\mu_{\mathrm{Elastic}}$) and ionic ($\Delta\mu_{\mathrm{Ion}}$) potentials as

$$\Delta\mu_{\mathrm{gel}} = \Delta\mu_{\mathrm{Mixing}} + \Delta\mu_{\mathrm{Elastic}} + \Delta\mu_{\mathrm{Ion}}. \tag{2}$$

If the swelling equilibrium is achieved, the chemical potential of the hydrogels is equal to that of the solvent in surrounding solution, i.e.,

$$\Delta\mu_{\mathrm{Mixing}} + \Delta\mu_{\mathrm{Elastic}} + \Delta\mu_{\mathrm{Ion}} = \Delta\mu^{*}_{\mathrm{Ion}}, \tag{3}$$

where $\Delta\mu^{*}_{\mathrm{Ion}}$ represents the chemical potential of solvent in the surrounding solution.

By the Flory–Huggins lattice theory [8], the change of mixing chemical potential due to the change of solvent–solvent contact into solvent–polymer contact is written mathematically as

$$\Delta\mu_{\mathrm{Mixing}} = \frac{k_{\mathrm{B}}T}{v}\left[\phi + \ln(1-\phi) + \chi\phi^{2}\right], \tag{4}$$

where k_B is the Boltzmann constant, T is the absolute temperature, v is the molar volume of the solvent, ϕ is the volume fraction of polymeric network at swelling equilibrium, and χ is the polymer–solvent interaction parameter. It is noted that the Flory–Huggins treatment of polymer solution is usually difficult for prediction of the behavior involved LCST. However, the computational approximation caused is generally acceptable. Furthermore, it is also known that the interaction parameter χ depends not only on the absolute temperature T but also on the volume fraction ϕ of polymeric network [9,14,22]. In the present MECtherm model, the following two forms of the polymer–solvent interaction parameters χ are used for different states of volume phase transition.

In the swelling state of the hydrogels with lower volume fraction ϕ of polymeric network below the lower critical solution temperature (LCST), the polymer–solvent interaction parameter χ is computed by

$$\chi = \chi_1(T) + \chi_2\phi = \frac{\delta h - \delta s T}{k_B T} + \chi_2\phi, \tag{5}$$

in which χ_2 is an empirical parameter. δs and δh are the changes of entropy and enthalpy per monomeric unit of the network, respectively.

In the shrinking state of the hydrogels with higher volume fraction ϕ of polymeric network above LCST, the polymer–solvent interaction parameter χ is computed by

$$\chi = F(T)P(\phi), \tag{6}$$

where $F(T)$ and $P(\phi)$ are the functions of absolute temperature T and volume fraction ϕ of polymeric network, respectively. Bae et al. defined $P(\phi)$ as [19]

$$P(\phi) = \frac{1}{1 - b\phi}, \tag{7}$$

in which b is an empirical parameter (here $b=0.65$). Hino and Prausnitz defined $F(T)$ as [14]

$$F(T) = \frac{z}{2}\left(\frac{\zeta + 2\zeta_{12}}{RT} + 2\ln\left(\frac{1 + s_{12}}{1 + s_{12}\exp(\zeta_{12}/(RT))}\right)\right), \tag{8}$$

where z is the lattice coordination number ($z=6$), ζ is the interchange energy, ζ_{12} is the difference between the segmental interaction energies of specific and non-specific interactions, R is the gas constant, and s_{12} is the degeneracy ratio of non-specific interactions to that of specific interactions.

In the numerical implementation, the transformation between Eqs. (5) and (6) is in fact determined by identifying the volume phase transition, when the difference of polymer volume fractions between the previously and currently iterating steps is much larger than the specified convergence region.

The contribution of elastic deformation of polymeric network matrix to the change of chemical potential is described by the affine model [8]

$$\Delta\mu_{\text{Elastic}} = k_B T v_e\left[\left(\frac{\phi}{\phi_0}\right)^{1/3} - \frac{\phi}{2\phi_0}\right], \tag{9}$$

where v_e is the effective crosslink density, ϕ_0 is the volume fraction of polymeric network in the pregel solution and ϕ_0/ϕ is the volume swelling ratio.

The ionic contribution to the change of chemical potential is determined by the concentration difference of mobile ions between the interior hydrogels and surrounding solution [8]

$$\Delta\mu_{\text{Ion}} - \Delta\mu^*_{\text{Ion}} = -k_B T\sum_j^N\left(c_j - c_j^*\right), \tag{10}$$

where N denotes the number of ionic species, c_j and c_j^* are the concentrations of mobile ions in the interior hydrogels and exterior bathing solution, respectively.

By substituting Eqs. (4), (9) and (10) into Eq. (3), the swelling equilibrium governing equation is obtained in form of transcendental equation as follows

$$\frac{\phi + \ln(1-\phi) + \chi\phi^2}{v} + v_e\left[\left(\frac{\phi}{\phi_0}\right)^{1/3} - \frac{\phi}{2\phi_0}\right] - \sum_j^N\left(c_j - c_j^*\right) = 0. \tag{11}$$

When the hydrogels are immersed into pure water, the ionic concentrations of the external solution are equal to zero. The swelling equilibrium governing Eq. (11) is then simplified into

$$\frac{\phi + \ln(1-\phi) + \chi\phi^2}{v} + v_e\left[\left(\frac{\phi}{\phi_0}\right)^{1/3} - \frac{\phi}{2\phi_0}\right] - c_f^0\frac{\phi}{\phi_0} = 0, \tag{12}$$

where c_f^0 is the fixed charge density at the reference state ($\phi=\phi_0$).

For incorporation of the diffusive ion concentrations and electric potential into the simulation of thermo-sensitive hydrogels, Poisson–Nernst–Planck system is employed. If the contributions of migration and diffusion to the transport of mobile ions are considered during thermal swelling, the steady-state Nernst–Planck equation for the kth ion species is expressed by [20]

$$D_k\nabla^2 c_k + \frac{FD_k z_k}{RT}\left(\nabla c_k\nabla\psi + c_k\nabla^2\psi\right) = 0, \quad (k = 1, 2, \ldots N) \tag{13}$$

where F is the Faraday constant and ψ is the electric potential. D_k, z_k and c_k are the diffusive coefficient, valence and concentration of the kth mobile ions, respectively.

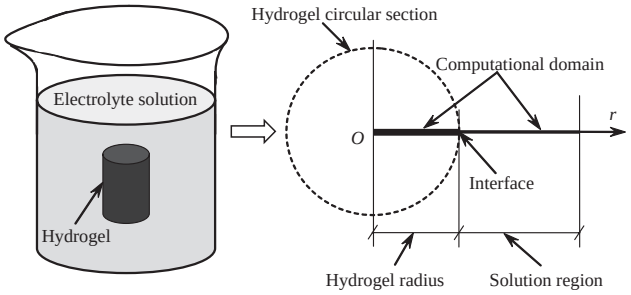

Fig. 1. A cylindrical hydrogel immersed in electrolyte solution. One-dimensional computational domain along radial direction covers both the hydrogel and bathing solution.

The corresponding Poisson equation for the electric potential is written as [20]

$$\nabla^2\psi = -\frac{F}{\varepsilon\varepsilon_0}\left(z_f c_f + \sum_k^N (z_k c_k)\right), \tag{14}$$

where ε_0 is the permittivity for vacuum, ε is the dielectric constant of medium relative to vacuum (ε=80 for water). z_f and c_f are the valence and density of fixed charges. It is reasonably assumed here that the fixed charges are uniformly attached to the polymeric network of the hydrogel matrix during thermal swelling and thus the total number of fixed charges is invariable, namely the fixed-charge density $c_f = c_f^0\phi/\phi_0$ at swelling equilibrium state. It is also noted that, in general, the Poisson–Boltzmann approach is more suitable to very low concentrations of univalent cations, which is one of limitations for the approach applications.

If an isotropic swelling is considered, the elongation ratios of the hydrogels are equal in each coordinate direction. The displacement vector $\boldsymbol{u}$ is then expressed by the difference between the deformed position $\boldsymbol{x}(\alpha x_0, \alpha y_0, \alpha z_0)$ and original position $\boldsymbol{x}(x_0, y_0, z_0)$, in which α is a linear ratio of volume swelling and $\alpha = (V/V_0)^{1/3} = (\phi_0/\phi)^{1/3}$,

$$\boldsymbol{u} = \boldsymbol{x} - \boldsymbol{x}_0 = \left[\left(\frac{\phi_0}{\phi}\right)^{1/3} - 1\right]\boldsymbol{x}_0. \tag{15}$$

In this paper, only cylindrical hydrogels are considered. Due to axisymmetry therefore, it is reasonable to use one-dimensional computational domain along the radial direction covering both the hydrogel radius and bathing solution, as shown in Fig. 1. The steady-state Nernst–Planck equations in the polar coordinates are thus simplified as

$$\frac{\partial^2 c_k}{\partial r^2} + \frac{1}{r}\frac{\partial c_k}{\partial r} + \frac{F z_k}{RT}\left(c_k\frac{\partial^2\psi}{\partial r^2} + \frac{c_k}{r}\frac{\partial\psi}{\partial r} + \frac{\partial c_k}{\partial r}\frac{\partial\psi}{\partial r}\right) = 0, \quad (k = 1, 2, \cdots N) \tag{16}$$

and the Poisson Equation is

$$\frac{\partial^2\psi}{\partial r^2} + \frac{1}{r}\frac{\partial\psi}{\partial r} = -\frac{F}{\varepsilon\varepsilon_0}\left(z_f c_f + \sum_k^N (z_k c_k)\right), \tag{17}$$

The radial displacement of the hydrogel is given by

$$u_r = \left[\left(\frac{\phi_0}{\phi}\right)^{1/3} - 1\right]R_0, \tag{18}$$

where R_0 is the radius of cylindrical hydrogel at the reference state.

As shown in Fig. 1, the boundary conditions required are applied at both the ends of 1-D computational domain. Due to axisymmetry of the present problem, the boundary conditions at the end point O of the circle centre are given as

$$\frac{\partial\psi}{\partial r} = 0 \quad \text{and} \quad \frac{\partial c_j}{\partial r} = 0 \qquad (j = 1, 2, \cdots N) \quad \text{at } r = 0 \tag{19}$$

The boundary conditions at the end point B of the solution region are given by

$$\psi = 0 \quad \text{and} \quad c_j = c^* \qquad (j = 1, 2, \cdots N) \quad \text{at } r = L. \tag{20}$$

3. Meshless Hermite–cloud method

The meshless Hermite–cloud method [18] is used here as a numerical tool for simulation of volume phase transition of the ionic thermo-sensitive hydrogels. The method is based on the Hermite interpolation theorem and the fixed kernel approximation, in which the approximation $\tilde{f}(x)$ of any one-dimensional unknown real function $f(x)$ is constructed by

$$\tilde{f}(x) = \sum_{n=1}^{N_T} N_n(x) f_n + \sum_{m=1}^{N_S}\left(x - \sum_{n=1}^{N_T} N_n(x) x_n\right) M_m(x) g_{xm}, \tag{21}$$

where N_T and N_S ($\leq N_T$) are total numbers of randomly scattered points covering both the interior computational domain and edges. f_n is the point value of unknown real function $f(x)$ at the nth point, and g_{xm} that of the first-order differential at the mth point. The corresponding discrete approximation is written as

$$\tilde{g}_x(x) = \sum_{m=1}^{N_s} M_m(x) g_{xm}. \tag{22}$$

In Eq. (21), the shape functions $N_n(x)$ and $M_m(x)$ of $f(x)$ and $g_x(x)$ are defined as [21]

$$N_n(x) = \boldsymbol{B}(u_n)\mathbf{A}^{-1}(x_k)\boldsymbol{B}^T(x)K(x_k - u_n)\Delta L_n, \quad (n = 1, 2, \ldots, N_T) \tag{23}$$

$$M_m(x) = \tilde{\boldsymbol{B}}(u_m)\tilde{\mathbf{A}}^{-1}(x_k)\tilde{\boldsymbol{B}}^T(x)K(x_k - u_m)\Delta L_m, \quad (m = 1, 2, \ldots, N_S) \tag{24}$$

in which ΔL_n is defined as the cloud length of the nth point, $\boldsymbol{B}(u)$ and $\tilde{\boldsymbol{B}}(u)$ are the linearly independent basis-function vectors as follows

$$\boldsymbol{B}(u) = \{b_1(u), b_2(u), b_3(u)\} = \{1, u, u^2\}, \tag{25}$$

$$\tilde{\boldsymbol{B}}(u) = \{b_1(u), b_2(u)\} = \{1, u\}, \tag{26}$$

and $\mathbf{A}(x_k)$ and $\tilde{\mathbf{A}}(x_k)$ are symmetric constant matrices associated with the central point x_k of the fixed cloud

$$\mathbf{A}_{ij}(x_k) = \sum_{n=1}^{N_T} b_i(u_n)K(x_k - u_n)b_j(u_n)\Delta L_n, \qquad (i,j = 1,2,3) \tag{27}$$

$$\tilde{\mathbf{A}}_{ij}(x_k) = \sum_{m=1}^{N_S} b_i(u_m)K(x_k - u_m)b_j(u_m)\Delta L_m, \qquad (i,j = 1,2) \tag{28}$$

where $K(x_k - u)$ is a kernel function constructed by cubic spline function as,

$$K(x_k - u) = \frac{1}{\Delta L_k}\begin{cases} 0 & 2 < z \\ (2-z)^3/6 & 1 \le z \le 2, \\ (2/3) - z^2(1 - z/2) & 0 \le z \le 1 \end{cases} \tag{29}$$

where $z = |(x_k - u)\Delta L_k|$.

Due to the additionally introduced unknown function $g_x(x)$, auxiliary condition is required. Imposing the first-order differential with respect to x on the approximation $\tilde{f}(x)$ (21) and considering Eq. (22), the auxiliary condition is obtained as

$$\sum_{n=1}^{N_T} N_{n,x}(x) f_n - \sum_{m=1}^{N_S}\left(\sum_{n=1}^{N_T} N_{n,x}(x)x_n\right) M_m(x) g_{xm} = 0, \tag{30}$$

where $N_{n,x}(x)$ denotes the first derivative of $N_n(x)$ with respect to the variable x.

The Hermite–cloud method is so far formulated. It is able to solve generic engineering differential boundary value problems as,

$$\boldsymbol{L}f(x) = P(x), \quad \text{PDEs in computational domain } \Omega \tag{31}$$

$$f(x) = Q(x), \quad \text{Dirichlet boundary conditionon } \Gamma_D \tag{32}$$

$$\partial f(x)/\partial n = R(x), \quad \text{Neumann boundary condition on } \Gamma_N \tag{33}$$

where $\boldsymbol{L}$ is differential operator and $f(x)$ unknown real function. By the point collocation technique, the approximation of the above problem is expressed in discrete form as

$$\boldsymbol{L}\tilde{f}(x_j) = P(x_j), \qquad (j = 1,2,\ldots,N_\Omega) \tag{34}$$

$$\tilde{f}(x_j) = Q(x_j), \qquad (j = 1,2,\ldots,N_D) \tag{35}$$

$$\partial\tilde{f}(x_j)/\partial n = R(x_j), \qquad (j = 1,2,\ldots,N_N) \tag{36}$$

where N_Ω, N_D and N_N are numbers of randomly scattered points in computational domain and along the Dirichlet and Neumann edges, respectively. Thus total number of the scattered points $N_T = N_\Omega + N_D + N_N$.

By substituting Eqs. (21) and (22) into Eqs. (34)–(36) and considering the auxiliary condition (30), a set of discrete algebraic equations with respect to unknown point values f_i and g_{xi} is derived in matrix form as

$$[H_{ij}]_{(N_T+N_S)\times(N_T+N_S)}\{F_i\}_{(N_T+N_S)\times 1} = \{d_i\}_{(N_T+N_S)\times 1}, \tag{37}$$

where $\{\boldsymbol{F}_i\}$ and $\{\boldsymbol{d}_i\}$ are (N_T+N_S)-order column vectors

$$\{\boldsymbol{F}_i\}_{(N_T+N_S)\times 1} = \left\{\{f_i\}_{1\times N_T}, \{g_{xi}\}_{1\times N_S}\right\}^T, \tag{38}$$

$$\{\boldsymbol{d}_i\}_{(N_T+N_S)\times 1} = \left\{\{P(x_i)\}_{1\times N_\Omega}, \{Q(x_i)\}_{1\times N_D}, \{R(x_i)\}_{1\times N_N}, \{0\}_{1\times N_S}\right\}^T, \tag{39}$$

and $[\mathbf{H}_{ij}]$ is a $(N_T+N_S)\times(N_T+N_S)$ coefficient matrix

$$[\mathbf{H}_{ij}] = \begin{bmatrix} [\boldsymbol{L}N_j(x_i)]_{N_\Omega\times N_T} & \left[\boldsymbol{L}\left(\left(x_i - \sum_{n=1}^{N_T} N_n(x_i)x_n\right)M_j(x_i)\right)\right]_{N_\Omega\times N_S} \\ [N_j(x_i)]_{N_D\times N_T} & [0]_{N_D\times N_S} \\ [0]_{N_N\times N_T} & [M_j(x_i)]_{N_N\times N_S} \\ [N_{j,x}(x_i)]_{N_S\times N_T} & \left[-\left(\sum_{n=1}^{N_T} N_{n,x}(x_i)x_n\right)M_j(x_i)\right]_{N_S\times N_S} \end{bmatrix}. \tag{40}$$

By solving the set of linear algebraic equations (37), (N_T+N_S) point values $\{\boldsymbol{F}_i\}$ are obtained. Accordingly, the approximate solution $\tilde{f}(x)$ and the first-order differential $\tilde{g}_x(x)$ are then computed through Eqs. (21) and (22), respectively.

4. Simulations and discussions

4.1. Numerical comparison with experiment

In order to examine the MECtherm model, a numerical comparison is made between the computed results and experimentally measured swelling data extracted from the published literature [1], where Hirotsu et al. [1] carried out the experiment of the ionic thermo-sensitive poly(*N*-isopropylacrylamide) (PNIPA) hydrogels immersed in pure water with changing temperature. As one of the typical thermo-sensitive biomaterials, the PNIPA hydrogel is well known due to its distinctive property of unique alteration between hydrophilic and hydrophobic character-

istics upon external temperature stimulation. When surrounding temperature is lower than the corresponding lower critical solution temperature (LCST), the PNIPA hydrogel behaves hydrophilic characteristics alluring more water since the hydrogen bonds form a stable shell around the hydrophobic groups. With increase of the external temperature, the hydrophobic characteristics appear to free the entrapped water molecules from the network as the hydrogen bond interactions become weakened or destroyed. When the temperature reaches to or is higher than the LCST, the hydrophobic interactions become fully dominant and then the hydrogel is thoroughly dehydrated. As the water releases, the polymer chains of the hydrogel collapse abruptly and the phase separation of the PNIPA hydrogel occurs, which is often termed the volume phase transition.

For simulation of the ionized PNIPA hydrogels immersed in pure water that Hirotsu et al. conducted experimentally [1], the governing Eq. (12) is required only and solved independently. For comparison with the experimental data, several experimental parameters of the ionized PNIPA hydrogels are taken as the input data of the simulations. They are the initially fixed charge density c_f^0=8 mM with the valence $z_f=-1$ and the initial volume fraction of polymeric network at the reference configuration ϕ_0=0.07. In the simulated temperature region, it is reasonably assumed that the change of the water density is negligibly small and then the effect of the change of the water density on the volume phase transition of PNIPA hydrogels is negligible. As such, the popularly specified constant v=18.0 cm^3/mol is taken as the water molar volume. In addition, the effective crosslink densities $v_e=1.4\times10^{-5}$ and 1.0×10^{-5} mol/cm^3 are taken for the hydrogels without and with the fixed charges, respectively. The polymer–solvent interaction parameter χ is calculated by Eqs. (5)–(8) based on the given data [1,14], in which $\delta s=-4.717\times10^{-23}$ J/K, $\delta h=-1.246\times10^{-20}$ J, ζ=0.698 kcal/mol and $\zeta_{12}/\zeta=-7$.

Fig. 2 shows the comparison between the computed results and the experimental data for the swelling equilibrium of the PNIPA hydrogels with and without fixed charges when immersed in pure water in the temperature range of 20–50 °C, in which very good agreement is achieved. It is also observed that the fixed charges attached onto the polymeric network enhance the swelling capability of the ionized hydrogels, and also increase the lower critical solution temperature (LCST), relatively compared with the case without the fixed charges. The unionized PNIPA hydrogels undergo a continuous volume phase transition at about temperature T=34.3 °C, while the ionized PNIPA hydrogels exhibit a discontinuous volume phase transition at about temperature T=35.6 °C. The temperature of volume phase transition of the ionized PNIPA hydrogel is thus about 1.3 °C higher than that of the unionized hydrogel. As the temperature increases, the volume swelling ratios of both the hydrogels decrease due to the shrinking behaviors. Furthermore, the curves of swelling equilibrium of both the hydrogels tend to be merged together at the temperature above 40 °C, where the hydrogels are almost fully dehydrated.

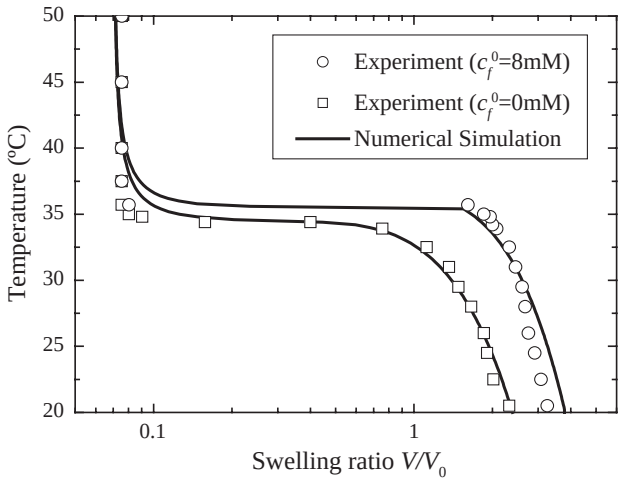

Fig. 2. Comparison of the present numerical simulations with the experimental swelling data [1] for the thermo-sensitive PNIPA hydrogels in pure water.

4.2. Study of the influence of the parameters on the ionized PNIPA hydrogels in univalent electrolyte solution

In the present parameter studies, the PNIPA hydrogels with the fixed charges are considered to be immersed in univalent electrolyte solution, instead of pure water. Several numerical studies are carried out for parameter studies on the responsive behaviors of the PNIPA hydrogels. The set of coupled nonlinear governing equations is solved iteratively, which consists of the swelling equilibrium Eq. (11), Nernst–Planck Eq. (16) and Poisson Eq. (17). By the truly meshless Hermite–cloud method, the set of the coupled nonlinear partial differential Eqs. (16) and (17) is firstly discretized into a set of nonlinear algebraic equations, and solved by the Newton's iterative technique for a guessed polymer-network volume fraction ϕ^*. The distributions of the electric potential and mobile ion concentrations are thus computed at a given temperature. Then by substituting the computed concentrations of mobile ions into the swelling equilibrium Eq. (11), the corresponding volume fraction ϕ of polymer network is obtained and used as the guessed value ϕ^* in next iterative step. In this way, the iterative recurrence is conducted until the convergence of volume fraction of polymer network. The algorithm is implemented for the parameter studies on the influences of the bathing solution concentration and polymeric-network crosslink density on the swelling equilibrium of the hydrogels with volume phase transition.

In general, before the swelling equilibrium is achieved, the thermo-sensitive ionized PNIPA hydrogels have a kinetic process of volume change. After the hydrogels are immersed into electrolyte bathing solution, the negatively

charged groups fixed to the network of polymeric chains are compensated by the cations diffusing into the hydrogel from the external solution where the constant concentrations of ion species are often assumed. The diffusion increases the cation concentration within the hydrogel and generates a concentration gradient between the hydrogel and bathing solution. The gradient is the source to generate the osmotic pressure to drive the kinetic swelling of the hydrogel. The initially fixed charge density c_f^0 plays an important role in the kinetics. When the density c_f^0 increases, the more cations diffuse into the hydrogels for compensation of the ionized network, which amplifies the magnitude of the concentration gradient. Then higher osmotic pressure is generated, which drives larger swelling of the hydrogels.

4.2.1. Influence of bathing solution concentration

For discussion of the influence of the bathing solution concentration c^* on the response behavior of the PNIPA hydrogels in swelling equilibrium, Figs. 3–7 are presented for the relationship between the swelling ratio V/V_0 and the temperature T, and the variations of the mobile ion concentrations c_k ($k=1,2,\ldots N$) and fixed charge density c_f as well as electric potential ψ along the radial coordinates for different c^* and T. Theoretically, for a thermo-sensitive ionized PNIPA hydrogel immersed in pure water, the swelling equilibrium state is achieved when the total osmotic pressure is equal to zero. However, this equilibrium state can be destroyed simply by introducing the electrolyte into the pure water, and then the kinetics of volume change undergoes until a new equilibrium is reached. At lower electrolyte concentration or in the special case of pure water, the negative charges of the PNIPA hydrogel network are neutralized by counter hydrogen ions. As the electrolyte concentration increases, the diffusive mobile cations from the bathing solution, instead of the hydrogen ions, are dominant within the PNIPA hydrogel. When the electrolyte concentration further increases, the cations and anions of the external solution diffuse more into the hydrogel and then the overall concentration of mobile ions within the hydrogel increases. However, the concentration difference is reduced between the interior hydrogel and exterior bathing solution, and consequently the driving force to swell the hydrogels decreases gradually, resulting in reduction of the swelling ratio V/V_0. It is also noted that the charge groups of the hydrogel network play a critical role in the hydrogel swelling. The electrostatic repulsion between neighboring charged groups along the hydrogel network acts to stiffen the chain and increase the swelling, which is the more notable effect at lower salt concentrations. In brief, with the increase of the bathing solution concentration c^*, the concentration gradient decreases. This causes smaller osmotic pressure and then drive lower swelling ratio V/V_0 of the hydrogels.

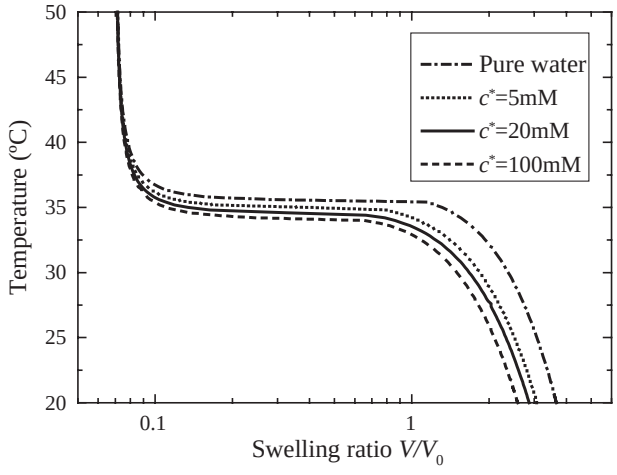

Fig. 3. Relation between the temperature T and swelling ratio V/V_0 of equilibrium volume for the ionized PNIPA hydrogels with initially fixed charge density c_f^0=5 mM when immersed in pure water and different bathing solution concentrations c^*=5, 20 and 100 mM, respectively.

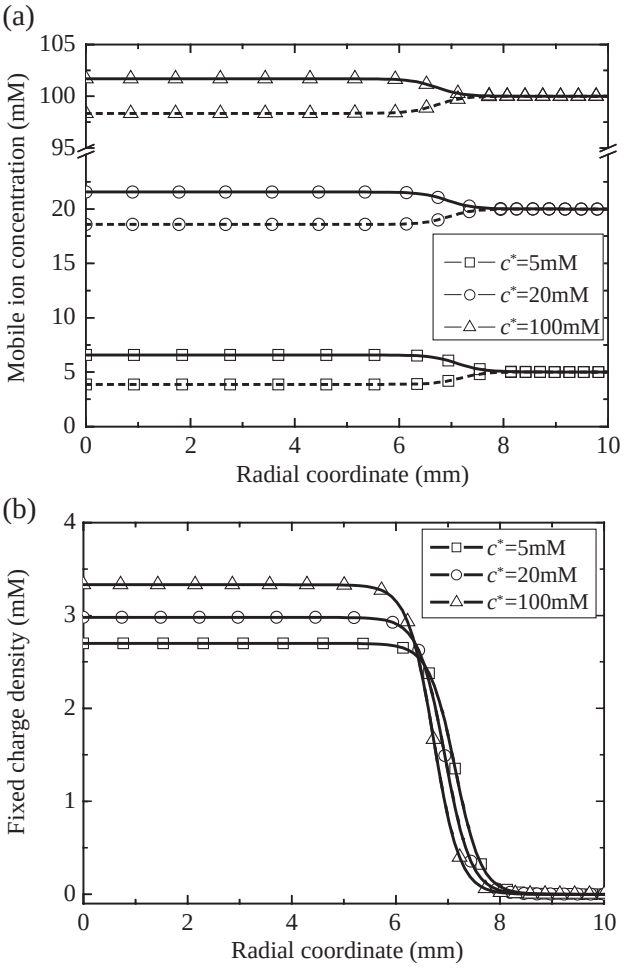

Fig. 4. Distributions of the mobile cation (solid line) and anion (dash line) concentrations (a), and the fixed charge density (b) versus radial coordinate for the ionized PNIPA hydrogels with initially fixed charge density c_f^0=5 mM when immersed in different bathing solution concentrations c^*=5, 20 and 100 mM at temperature T=30 °C.

In the present simulations, the thermo-sensitive ionized PNIPA hydrogels with initially fixed charge density c_f^0=5 mM are studied for discussions of the influences of ionic

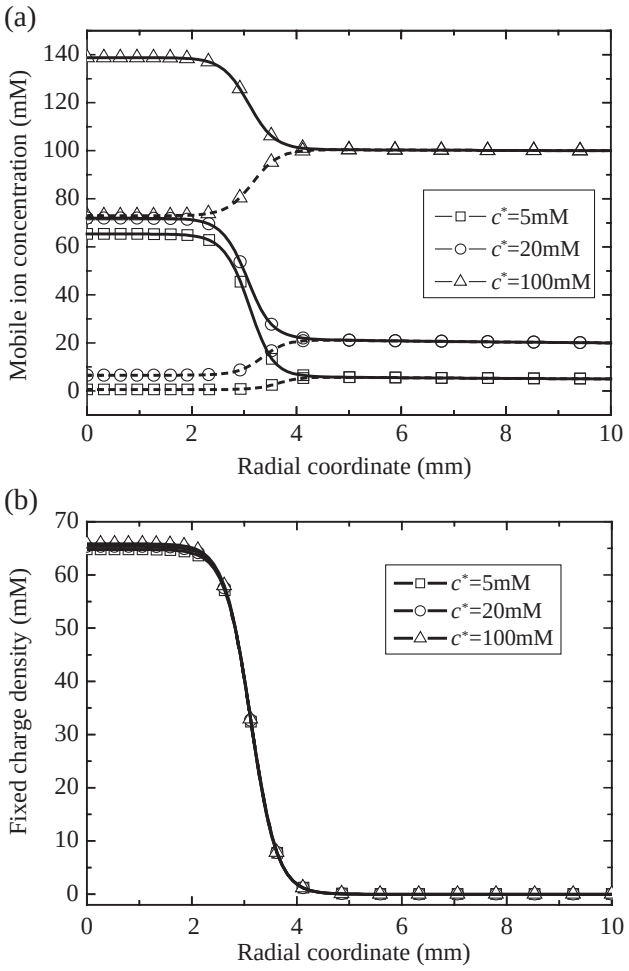

Fig. 5. Distributions of the mobile cation (solid line) and anion (dash line) concentrations (a) and the fixed charge density (b) versus radial coordinate for the ionized PNIPA hydrogels with initially fixed charge density c_f^0=5 mM when immersed in different bathing solution concentrations c^*=5, 20 and 100 mM at temperature T=40 °C.

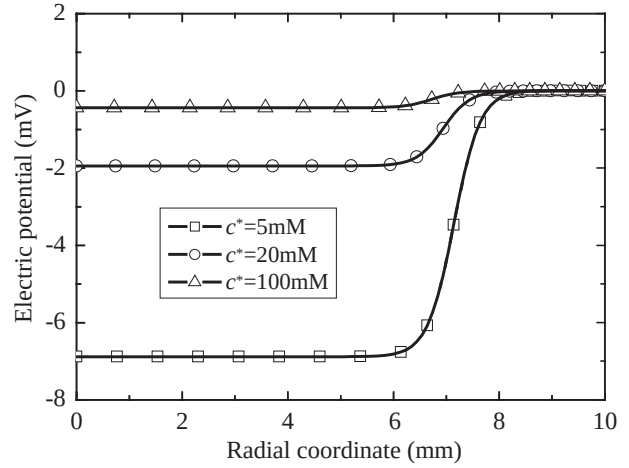

Fig. 6. Distributions of electric potentials ψ versus radial coordinate for the ionized PNIPA hydrogels with initially fixed charge density cf^0=5 mM when immersed in different bathing solution concentrations c^*=5, 20 and 100 mM at temperature T=30 °C.

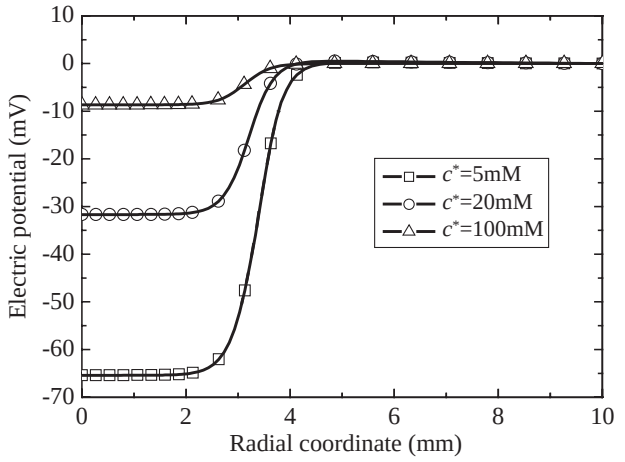

Fig. 7. Distributions of electric potentials ψ versus radial coordinate for the ionized PNIPA hydrogels with initially fixed charge density c_f^0=5 mM when immersed in different bathing solution concentrations c^*=5, 20 and 100 mM at temperature T=40 °C.

concentration c^* of bathing solution on swelling behavior. Fig. 3 shows the variations of the swelling ratio V/V_0 of the hydrogels with environmental temperature T at different bathing solution concentrations c^*=0 (pure water), 5, 20 and 100 mM, respectively. It is observed from the figure that simulations verify the above theoretical analysis, in which the PNIPA hydrogels placed in pure water have the larger swelling ratio V/V_0 than those in electrolyte solution. With increasing the ionic concentration c^* of bathing solution, the swelling ratio V/V_0 decreases and the temperature of volume phase transition also decreases. When the temperature T reaches to above 40 °C, the hydrogels become completely dehydrated regardless of the ionic concentration c^* of bathing solution.

In order to study the influences of the environmental temperature T and bathing solution concentration c^* on the distributions of mobile ion concentrations c_k, fixed charge density c_f and electric potentials ψ in swelling equilibrium, Figs. 4–7 are plotted for the ionized cylindrical PNIPA hydrogels immersed in different univalent electrolyte bathing solutions, in which the radial coordinate represents the one-dimensional computational domain along the radial direction covering both the cylinder hydrogel radius and bathing solution, and the sudden changes of the curves are observed at the interface between the hydrogel and solution.

The concentration distributions of the mobile cation and anion in the interior hydrogels and exterior bathing solution are plotted in Fig. 4(a) at temperature T=30 °C and Fig. 5(a) at temperature T=40 °C. The distributions of fixed charge density c_f in swelling equilibrium are shown in Fig. 4(b) at T=30 °C and Fig. 5(b) at T=40 °C, respectively. It is seen from Figs. 4(a) and 5(a) that, for a given concentration c^* of electrolyte bathing solution, the concentration of mobile cation in the PNIPA hydrogels at temperature T=40 °C is higher than that at T=30 °C, but the opposite trend is observed for the concentration of mobile anion. At a given

environmental temperature T, with increasing the concentration c^* of bathing solution, the mobile cation concentration increases in the PNIPA hydrogels, while the mobile anion concentration decreases. As the ionic concentration c^* of bathing solution increases, the difference of mobile ion concentrations decreases between the interior hydrogel and exterior solution. Figs. 4 and 5 also demonstrate the phenomena that all the concentrations of mobile ions and fixed charge are compensated.

The distributions of the electric potentials ψ in both the interior hydrogels and exterior bathing solution are shown in Fig. 6 at $T=30$ °C and Fig. 7 at $T=40$ °C, respectively. For a given concentration c^* of electrolyte bathing solution, the electric potential ψ within the PNIPA hydrogels at temperature $T=30$ °C is much higher than that at $T=40$ °C. For a given environmental temperature T, the electric potential ψ within the PNIPA hydrogels increases with the ionic concentration c^* of electrolyte bathing solution.

4.2.2. Influence of effective crosslink density

For analysis of the influence of crosslink density of polymeric network, Fig. 8 is presented for the relations between the temperature T and swelling ratio V/V_0 with different effective crosslink densities v_e. Figs. 9–12 illustrate the distributions of the mobile ionic concentrations c_k ($k=1,2,\ldots N$), fixed charge density c_f and electric potential ψ with different v_e and T. As well known, a crosslinker substance can induce the crosslink as the chemical bonds between linear polymeric molecules, and lead to form polymeric networks. The formed crosslink divides long chains into short chains connecting each other and thus forms numerous pores inside the hydrogels. Usually the hydrogels in large expansion state contain a large amount of water in the pores. In swelling equilibrium state, the water uptake mostly depends on the crosslink density. As the crosslink density increases, the polymeric network becomes stiffer, the pore size becomes smaller, and the water uptake decreases. Therefore, the increase of the crosslink density reduces the porous volume of the hydrogel network structure, and provides smaller space for water uptake, which leads to a lower swelling ratio in equilibrium state.

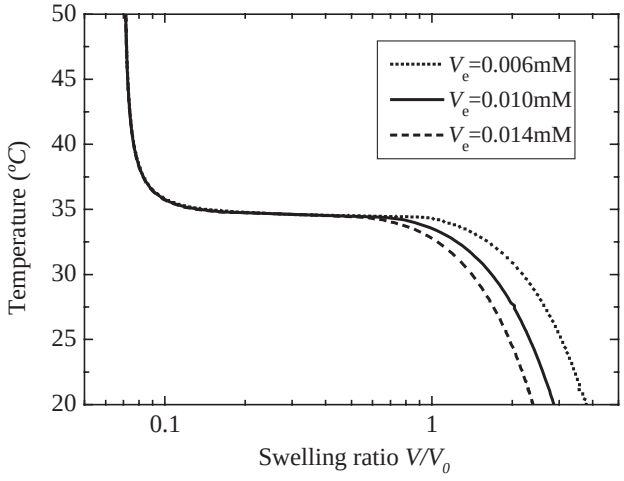

Fig. 8. Relation between the temperature T and swelling ratio V/V_0 of equilibrium volume for the ionized hydrogels with initially fixed charge density $c_f^0=5$ mM and different crosslink densities $v_e=0.006$, 0.010 and 0.014 mM when immersed in the univalent electrolyte solution $c^*=20$ mM.

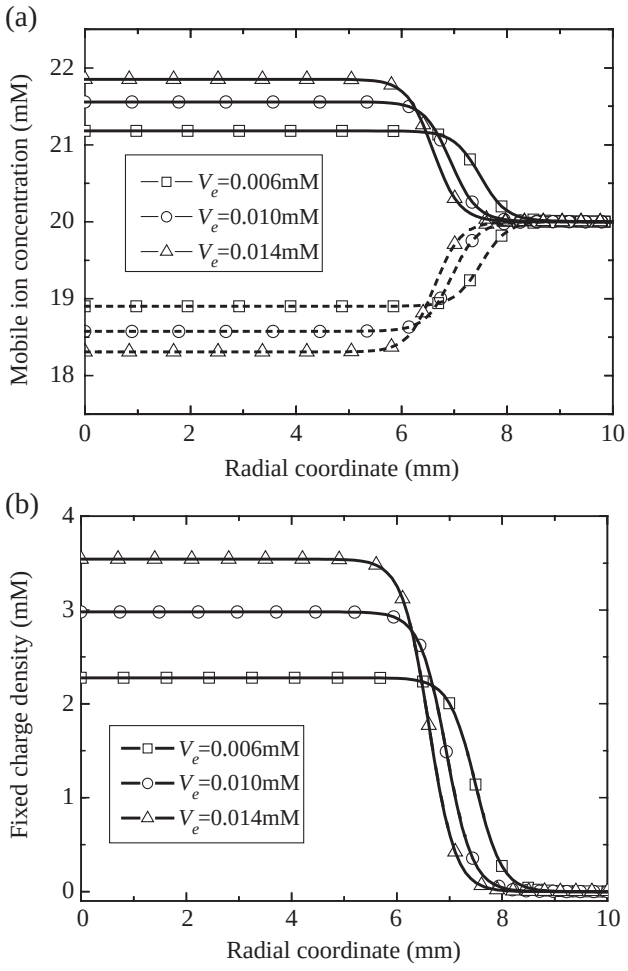

Fig. 9. Distributions of the mobile cation (solid line) and anion (dash line) concentrations (a) and the fixed charge density (b) versus radial coordinate for the ionized PNIPA hydrogels with initially fixed charge density $c_f^0=5$ mM and different crosslink densities $v_e=0.006$, 0.010 and 0.014 mM when immersed in the univalent electrolyte solution $c^*=20$ mM at temperature $T=30$ °C.

In the simulations to investigate the influences of effective crosslink density v_e on variations of the swelling ratio V/V_0 in equilibrium state with environmental temperature T, as shown in Fig. 8, three thermo-sensitive ionized PNIPA hydrogels with the initially fixed charge density $c_f^0=5$ mM are considered for different effective crosslink densities $v_e=0.006$, 0.010 and 0.014 mM, respectively, when the hydrogels are immersed in univalent electrolyte bathing solution $c^*=20$ mM. It is seen from the figure that, regardless of the crosslink densities v_e, the swelling ratios V_0/V of the equilibrium thermo-sensitive PNIPA hydrogels have similar profiles as a function of temperature T. The LCSTs or the volume phase transition temperatures are

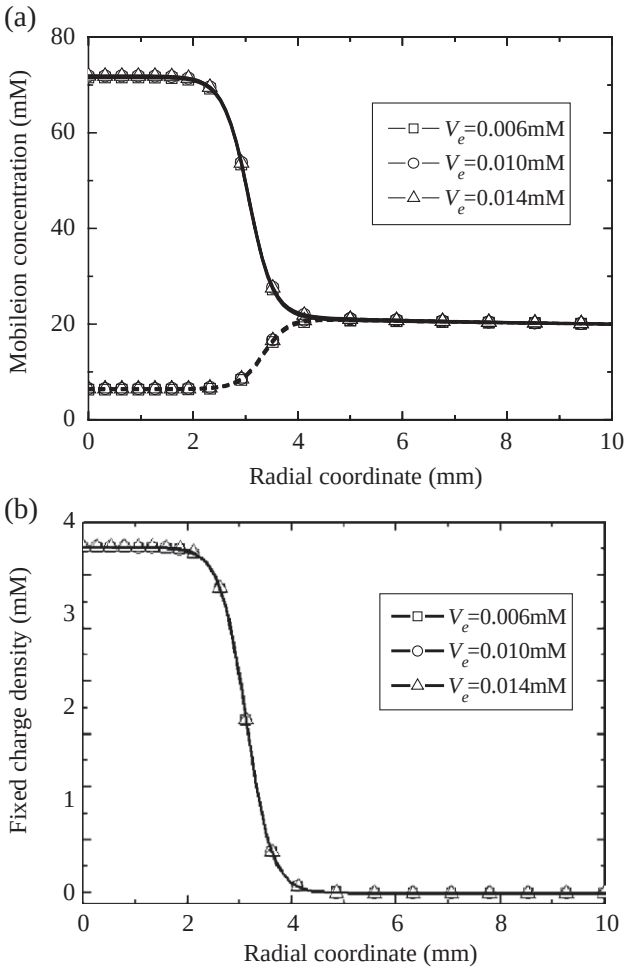

Fig. 10. Distributions of the mobile cation (solid line) and anion (dash line) concentrations (a), and the fixed charge density (b) versus radial coordinate for the ionized PNIPA hydrogels with initially fixed charge density c_f^0=5 mM and different crosslink densities v_e=0.006, 0.010 and 0.014 mM when immersed in the univalent electrolyte solution c^*=20 mM at temperature T=40 °C.

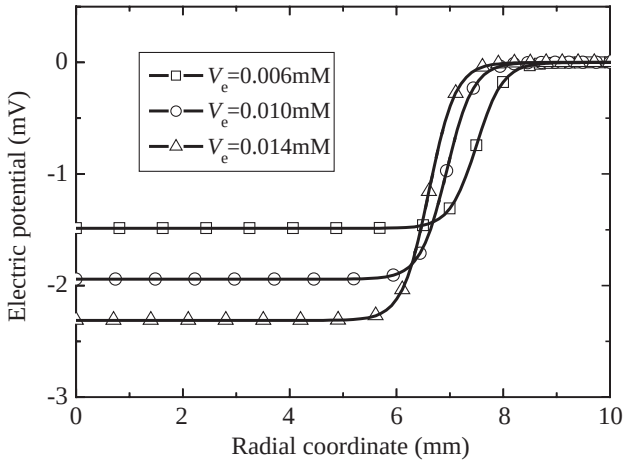

Fig. 11. Distributions of electric potentials ψ versus radial coordinate for the ionized PNIPA hydrogels with initially fixed charge density c_f^0=5 mM and different crosslink densities v_e=0.006, 0.010 and 0.014 mM when immersed in the univalent electrolyte solutions c^*=20 mM at temperature T=30 °C.

almost same for the three hydrogels, in which all lie in the vicinity of 34.6 °C. It is also known from Fig. 8 that, at the temperature below LCST, the volume swelling ratio V/V_0 of the equilibrium PNIPA hydrogel with the effective crosslink density v_e=0.010 mM is larger than that with larger v_e=0.014 mM, and smaller than that with lower v_e=0.006 mM. The volume changes of the equilibrium hydrogels with lower crosslink density v_e are thus larger than those with higher crosslink density v_e at temperatures below LCST.

In order to study the influence of the environmental temperature T and effective crosslink density v_e on the distributions of the mobile ion concentrations c_k, fixed charge density c_f and electric potential ψ along the radial coordinate in swelling equilibrium state, Figs. 9–12 are plotted for the ionized cylindrical PNIPA hydrogels immersed in the univalent electrolyte bathing solution, in which the radial coordinate represents the one-dimensional computational domain along the radial direction covering both the cylinder hydrogel radius and bathing solution, and the sudden changes of the curves are observed at the interface between the hydrogel and solution.

The concentration distributions of the mobile cation and anion in both the interior hydrogels and exterior bathing solution are demonstrated in Fig. 9(a) at temperature T=30 °C and Fig. 10(a) at temperature T=40 °C. Correspondingly, the distributions of fixed charge density c_f in equilibrium state are plotted in Fig. 9(b) at T=30 °C and Fig. 10(b) at T=40 °C. Figs. 9(a) and 10(a) show that, for a given effective crosslink density v_e, the mobile cation concentration in the interior PNIPA hydrogels at temperature T=40 °C is much higher than that at T=30 °C, which is caused by depleting water from the hydrogels due to the

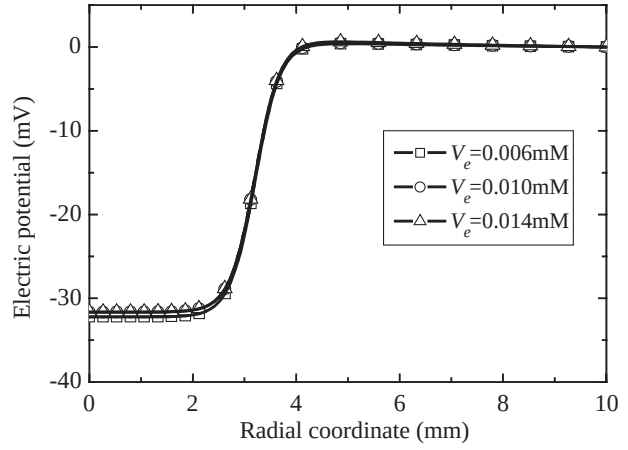

Fig. 12. Distributions of electric potentials ψ versus radial coordinate for the ionized PNIPA hydrogels with initially fixed charge density c_f^0=5 mM and different crosslink densities v_e=0.006, 0.010 and 0.014 mM when immersed in the univalent electrolyte solution c^*=20 mM at temperature T=40 °C.

collapse. At temperature $T=30$ °C, the mobile cation concentration in the interior PNIPA hydrogels increases with the effective crosslink density v_e. The opposite trends are observed for the mobile anion concentration. As the effective crosslink density v_e increases, the mobile anion concentration decreases. In addition, the increase of the effective crosslink density v_e makes the larger difference of ionic concentrations between the interior hydrogel and exterior solution. At temperature $T=40$ °C, all mobile ion concentrations in both the hydrogels and solution are equal to each other for different crosslink densities v_e, which is the result of the same swelling ratio as portrayed in Fig. 8. Figs. 9 and 10 demonstrate similar phenomena that all the concentrations of mobile cation and anion as well as fixed charges are compensated.

The distributions of the electric potential ψ in both the interior hydrogels and exterior bathing solution are illustrated in Fig. 11 at temperature $T=30$ °C and Fig. 12 at temperature $T=40$ °C. For a given effective crosslink density v_e, the electric potential ψ in the PNIPA hydrogel at temperature $T=30$ °C is much higher than that at $T=40$ °C. At the temperature T below the volume phase transition temperature such as $T=30$ °C, the electric potential ψ in the PNIPA hydrogels decreases with increasing the effective crosslink density v_e. At the temperature above the volume phase transition temperature such as $T=40$ °C, the electrical potentials ψ for different effective crosslink densities v_e are equal in both the hydrogels and solution, similarly because of the same swelling ratio V/V_0.

5. Conclusions

In this paper, the swelling equilibrium of ionic thermosensitive hydrogels with volume phase transition has been investigated when the hydrogels are immersed in bathing solution with changing temperature. The influences of the bathing solution concentration and crosslink density of polymeric network on the swelling equilibrium have been modeled and simulated through the multiphysics model, called the multi-effect-coupling thermal-stimulus (MECtherm) model. It consists of the Poisson–Nernst–Planck nonlinear partial differential system and swelling equilibrium transcendental governing equation. The MECtherm model is examined by one-dimensional meshless numerical comparison with experimental data for a cylindrical thermosensitive poly(*N*-isopropylacrylamide) (PNIPA) hydrogel, and very good agreement is achieved. Several parameter studies are conducted to discuss the influences of environmental temperature and bathing solution concentration as well as crosslink density of polymeric network on the swelling equilibrium of the hydrogels. Simulation predicts quantitatively that the swelling capability of the hydrogels increases with decreasing the bathing solution concentration or with decreasing the crosslink density of polymeric network.

Acknowledgements

The authors gratefully acknowledge the financial support from the Agency for Science, Technology and Research (A*STAR) of Singapore through A*STAR SERC Grant-SRP on MEMS Phase II under the project number: 022 107 0009.

References

[1] S. Hirotsu, Y. Hirokawa, T. Tanaka, Volume-phase transitions of ionized *N*-isopropylacrylamide gels, J. Chem. Phys. 87 (1987) 1392–1395.
[2] H. Feil, Y.H. Bae, J. Feijen, S.W. Kim, Mutual influence of pH and temperature on the swelling of ionizable and thermosensitive hydrogels, Macromolecules 25 (1992) 5528–5530.
[3] I. Ohmine, T. Tanaka, Salt effects on the phase transition of ionic gels, J. Chem. Phys. 77 (1982) 5725–5729.
[4] X. Zhou, Y.C. Hon, S. Sun, A.F.T. Mak, Numerical simulation of the steady-state deformation of a smart hydrogel under an external electric field, Smart Mater. Struct. 11 (2002) 459–467.
[5] H. Yu, D.W. Grainger, Thermo-sensitive swelling behavior in crosslinked *N*-isopropylacrylamide networks: cationic, anionic, and ampholytic hydrogels, J. Appl. Polym. Sci. 49 (1993) 1553–1563.
[6] R.F.S. Freitas, E.L. Cussler, Temperature sensitive gels as extraction solvents, Chem. Eng. Sci. 42 (1987) 97–103.
[7] Y. Li, T. Tanaka, Phase transitions of gels, Annu. Rev. Mater. Sci. 22 (1992) 243–276.
[8] P.J. Flory, Principles of Polymer Chemistry, Cornell University Press, Ithaca, NY, 1953.
[9] H. Shirota, N. Endo, K. Horie, Volume phase transition of polymer gel in water and heavy water, Chem. Phys. 238 (1998) 487–494.
[10] T. Tanaka, D. Fillmore, S.T. Sun, I. Nishio, G. Swislow, A. Shah, Phase transitions in ionic gels, Phys. Rev. Lett. 45 (1980) 1636–1639.
[11] A.K. Lele, M.V. Badiger, M.M. Hirve, R.A. Mashelkar, Thermodynamics of hydrogen-bonded polymer gel–solvent systems, Chem. Eng. Sci. 50 (1995) 3535–3542.
[12] K. Otake, H. Inomata, M. Konno, S. Saito, A new model for the thermally induced volume phase transition of gels, J. Chem. Phys. 91 (1989) 1345–1350.
[13] B. Erman, P.J. Flory, Critical phenomena and transitions in swollen polymer networks and in linear macromolecules, Macromolecules 19 (1986) 2342–2353.
[14] T. Hino, J.M. Prausnitz, Molecular thermodynamics for volume-change transitions in temperature-sensitive polymer gels, Polymer 39 (1998) 3279–3283.
[15] T.M. Birshtein, V.A. Pryamitsyn, Coil–globule type transitions in polymers. 2. Theory of coil–globule transition in linear macromolecules, Macromolecules 24 (1991) 1554–1560.
[16] B.G. Ten, F.E. Karasz, Lower critical solution temperature behavior in polymer blends: compressibility and directional-specific interactions, Macromolecules 17 (1984) 815–820.
[17] H. Li, X.G. Wang, G.P. Yan, K.Y. Lam, S.X. Cheng, T. Zou, R.X. Zhuo, A novel multiphysic model for simulation of swelling equilibrium of ionized thermal-stimulus responsive hydrogels, Chem. Phys. 309 (2005) 201–208.
[18] H. Li, T.Y. Ng, J.Q. Cheng, K.Y. Lam, Hermite–cloud: a novel true meshless method, Comput. Mech. 33 (2003) 30–41.
[19] Y.C. Bae, J.J. Shim, D.S. Soane, J.M. Prausnitz, Representation of vapor–liquid and liquid–liquid equilibria for binary systems containing polymers: applicability of an extended Flory–Huggins equation, J. Appl. Polym. Sci. 47 (1993) 1193–1206.

[20] E. Samson, J. Marchand, J.L. Robert, J.P. Bournazel, Modelling ion diffusion mechanisms in porous media, Int. J. Numer. Methods Eng. 46 (1999) 2043–2060.
[21] T.Y. Ng, H. Li, J.Q. Cheng, K.Y. Lam, A new hybrid meshless-differential order reduction (hM-DOR) method with applications to shape control of smart structures via distributed sensors/actuators, Eng. Struct. 25 (2003) 141–154.
[22] R. Moerkerke, R. Koningsveld, H. Berghmans, K. Dusek, K. Solc, Phase transitions in swollen networks, Macromolecules 28 (1995) 1103–1107.